Functionalization of Pt(IV)–Ammines Enables Site-Directed Covalent Modification of mRNA

Edward Miller, Charlotte E. Farquhar, Jacob Rodriguez, Andrei Loas, Bradley L. Pentelute*

Massachusetts Institute of Technology, Department of Chemistry, Cambridge, Massachusetts 02139, United States

Supporting Information Placeholder

ABSTRACT: Developing chemical toolkits for mRNA modification has remained an immense challenge driven by inherent difficulties in targeting mRNA molecules. Antisense oligonucleotides (ASOs) offer a promising framework for targeting specific mRNA sequences, yet they do not possess the capacity to alter the covalent structure of mRNA except through enzyme-mediated hydrolysis. The requirement of relying on an enzyme for modifying mRNA incurs several limitations on the application, design, and delivery of ASOs. To address these limitations, we developed a Pt(IV)-ASO strategy that combines the reactivity of platinum with the sequence specificity of ASOs to covalently modify nucleic acids, including short RNA and mRNA, in a selective, enzyme-free manner. Access to Pt(IV)-ASO constructs was made possible by an innovative equatorial Pt(IV) ammine functionalization strategy, allowing for conjugation of carboxylic acids directly to the Pt core. Reactivity with 21-mer RNA and full-length mRNA by Pt-ASO constructs was demonstrated, and the covalently modified products were characterized using a suite of orthogonal techniques, such as electrophoretic mobility shift assay, MALDI-TOF MS, temperature-dependent dissociation assay, and RT-qPCR. Constructs were optimized for their reactivity and selectivity, allowing for Pt(IV)-PMO constructs with sub-nanomolar IC_{50} values in an RNA competition assay. This Pt(IV)-ASO platform facilitates new avenues for RNA modification by providing a strategy for covalent modification of nucleic acids with potential applications for molecular biology research.

Introduction

Extensive work has been dedicated to developing diverse chemical toolkits to attenuate and enhance the function of proteins, including discovery of binders,[1–4] development of site- and chemoselective bioconjugation reactions,[5] and designing proteolysis targeting chimeras (PROTACs) to degrade proteins.[6] Despite mRNA being the progenitor of proteins, a similar complementary chemical toolkit for modifying native mRNA is not available. This lack of suitable functionalization methods is primarily due to the inherent challenges of targeting mRNA. Unlike proteins, which are built from a diverse set of 20 amino acid monomers and have a wide range of structural complexities, mRNAs consist of only four nucleotide monomers and exhibit limited diversity in their tertiary structure. The most successful approaches for selectively targeting mRNA are based on antisense oligonucleotides (ASOs), which are short single stranded synthetic oligomers designed to bind mRNA through base-pairing. ASOs are an expanding class of FDA-approved therapeutics that restore proper gene expression through two mechanisms: RNA cleavage and RNA blockage.[7]

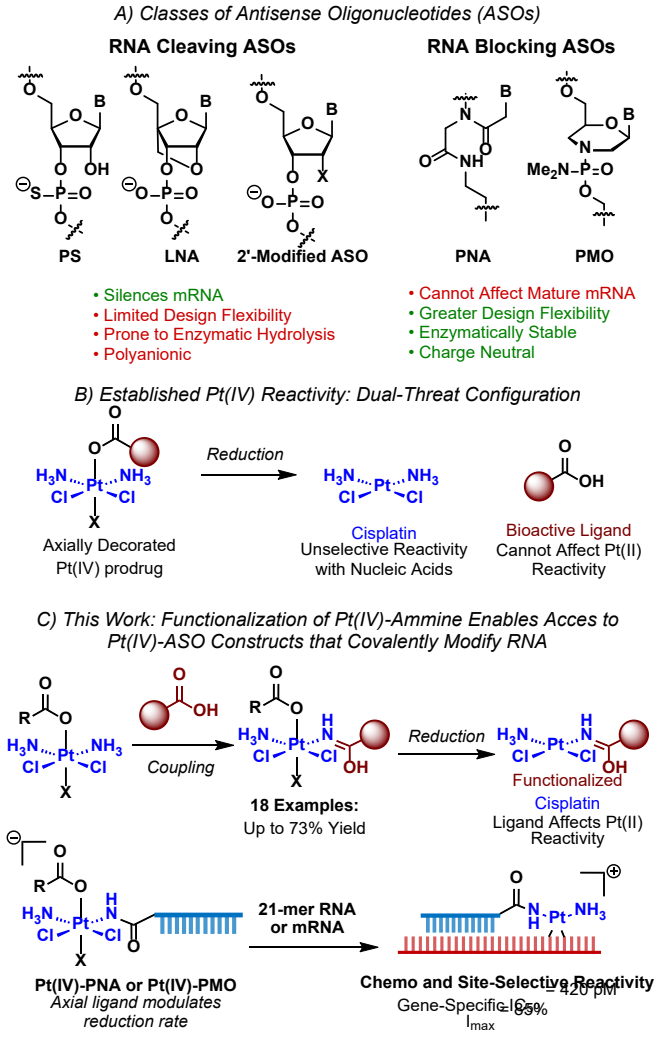

Figure 1. ASO architectures and Pt(IV) prodrug synthesis/reactivity. (A) Prevalent ASO architectures. (B) Established "dual-threat" design of Pt(IV)-prodrugs. (C) Development of a late-stage equatorial Pt(IV)–ammine functionalization strategy for accessing Pt(IV)-ASOs that can covalently modify RNA in a site-directed manner. Half-maximal inhibitory concentration ($1C_{50}$) and maximum drug inhibition (I_{max}) determined via competition assay

Included in the class of mRNA cleaving ASOs are phosphorothioate oligonucleotides (PS),[8–11] locked nucleic acids (LNA),[12–14] and 2' ribose modified ASOs (**Fig 1A**).[15–19] These ASOs bind mRNA to form a duplex mimicking RNase H1's native substrate. After recognition by RNase H1 present in the proteome, the mRNA is subsequently cleaved, leading to targeted mRNA degradation.[20] The reliance on an enzyme-based mechanism to silence mRNA incurs several inherent limitations onto the design of these ASO, as they must balance nuclease recognition with enzymatic stability. Additionally, their polyanionic nature renders them cell impermeable, a major obstacle for delivery, requiring the addition of targeting ligands or lipid nanoparticles to facilitate transport into the cell.[21]

Complementary to this class of ASOs are those which exert their biological effect through steric hindrance. Included in this class are peptide nucleic acids (PNAs)[22,23] and phosphorodiamidate morpholino oligonucleotide (PMOs),[24] which have been FDA approved for the treatment of neurodegenerative diseases via splice correction.[25–27] They are proteolytically stable, feature high binding affinity to their antisense sequence, and are charge neutral, thus displaying higher binding affinity to RNA than enzyme engaging ASOs.[28] As a result of their non-biological structure, these ASOs are not recognized by native enzymes, and thus, cannot affect mature mRNA function.

Due to the inherent limitations of current ASOs, identifying an approach to functionalize mRNA independently of enzyme-based pathways was identified as an unmet challenge.[29] We proposed to address this challenge by tethering a covalent warhead to an ASO, which would modify its target mRNA after binding. A platinum-based warhead was identified as the ideal electrophile to use for a covalent modification strategy of mRNA.[30] Platinum's inherent reactivity towards nucleic acids, specifically DNA, has led to platinum-containing drugs becoming a crucial class of chemotherapies.[31] Amongst this class, cisplatin, carboplatin, and oxaliplatin are the most prescribed, and are approved worldwide to treat multiple forms of cancer.[32] These compounds covalently react with DNA to form intrastrand adducts between two neighboring guanosines, which serve as haltsites for DNA transcription.[33] Leveraging this reactivity for mRNA, it was hypothesized that similar lesions could be formed with mRNA that would inhibit its translation, paving way for this approach to be used for both mRNA modification and mRNA silencing.

Here, we report a coupling strategy between activated carboxylic acids and Pt(IV)–ammines, tolerating a variety of Pt(IV)-prodrugs and biologically relevant carboxylic acids (**Fig. 1C**). This transformation enabled access to Pt(IV)-PNA and Pt(IV)-PMO constructs that can site-selectively modify mRNA. We demonstrate that this covalent modification serves as a lesion, rendering the mRNA unable to be fully processed by mRNA engaging enzymes, effectively silencing it.

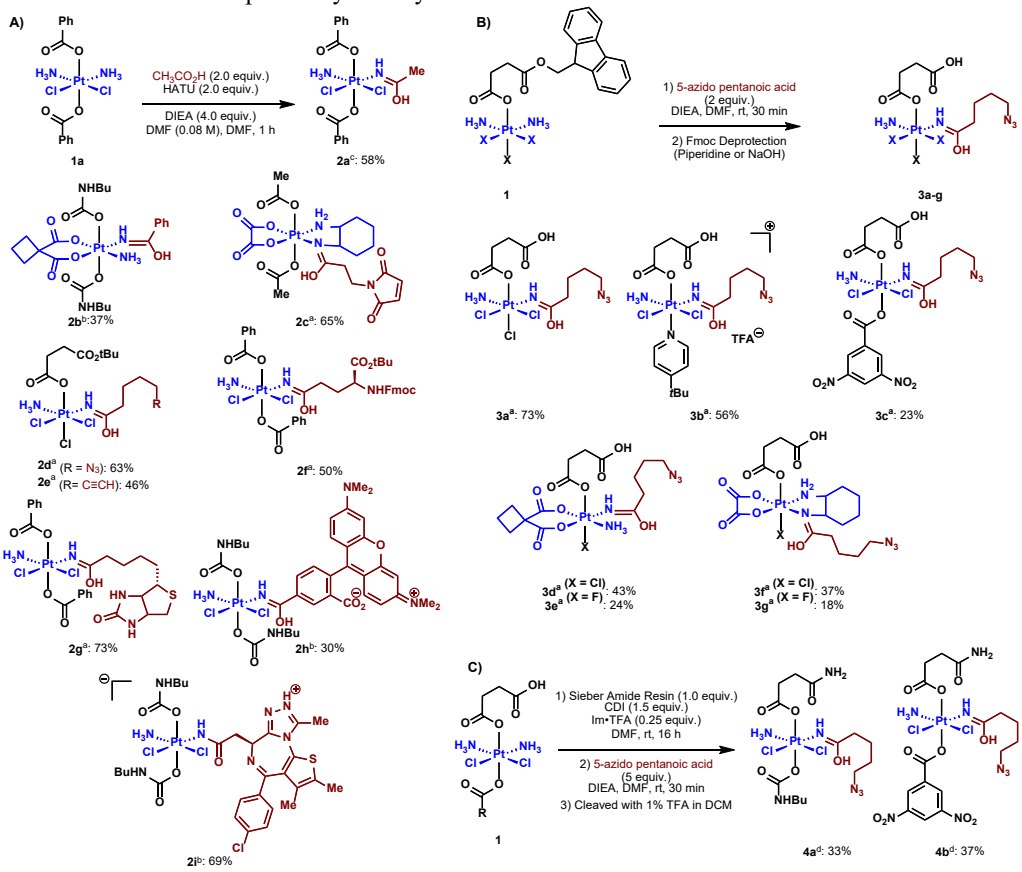

Figure 2. Scope of Pt(IV)–Ammine Functionalization Pt-Ammine functionalization is successful across a broad scope of biologically relevant coupling partners. (A) Solution-phase coupling of Pt(IV)-compounds with carboxylic acids. (B) Two-step procedure for accessing Pt(IV)–amide complexes with pendant carboxylic acids. (C) Solid-phase coupling of Pt(IV)-compounds with carboxylic acids. [a]Conditions: **1** (0.10 mmol, 1.0 equiv), RCO_2H (2.0 equiv), HATU (2.0 equiv), DIEA (4.0 equiv), DMF (1.25 mL), rt, 1 h. [b]Conditions: **1** (0.10 mmol, 1.0 equiv), RCO_2H (2.0 equiv), HATU (2.0 equiv), DIEA (8.0 equiv), DMF (625 µL), rt, 1 h. [c]Reaction performed using standard conditions "a" on 0.5 mmol scale. [d]Conditions: 1) **1** (0.15 mmol, 1.5 equiv), CDI (1.5 equiv), Sieber Amide Resin (1.0 equiv), Imidazole•TFA (0.25 equiv), DMF (920 µL), rt, 16 h. 2) 5-azido pentanoic acid (5.0 equiv), HATU (5.0 equiv), DIEA (260 µL), DMF (1.3 mL), rt, 30 min. Yields are of isolated **2a–2i**, **3a-g**, and **4a-b**.

Results and Discussion

Engineering a platinum reagent for a targeted covalent modification strategy is streamlined by the modularity of its primary coordination sphere, which allows for tuning of physical and chemical properties.[34] Pt(IV)-prodrugs are extensively researched due to their stability towards hydrolysis in the extracellular environment and their ability to be readily reduced intracellularly to bioactive Pt(II) compounds. Numerous applications have been explored with the Pt(IV) architecture via installation of bioactive ligands to the reductively labile axial positions (**Fig. 1B**).[35–44] While this "dual-threat" strategy is well-established, an mRNA targeting approach would require that the targeting ASO remains attached upon reduction in order to position the Pt(II) core for targeted reactivity with mRNA. To accomplish this feature, the ASO would need to be appended to a reductively non-labile (L-type) coordination site of the Pt(IV). This "synergistic" configuration is significantly less studied than the "dual-threat" configuration, due to the lack of methods to functionalize these equatorial L-type ligands in Pt(IV) compounds in a late-stage manner.

Taking inspiration from the reported reactivity of transition metal– ammine complexes with electrophiles,[45–50] we hypothesized that treatment of a Pt(IV)–ammine with an activated carboxylic acid could be a suitable approach to functionalize the Pt-core. To explore this hypothesis, the reactivity of Pt(IV) complex **1a** with 1-[bis(dimethylamino)methylene]-1H-1,2,3-triazolo[4,5-b]pyrdinium 3-oxide hexafluorophosphate (HATU)-activated acetic acid under basic conditions was examined (**Fig. 2A)**. Under these reaction conditions, formation of the functionalized product **2a** was observed in good yield (58%). Functionalization of the ammine was supported by ^{195}Pt-^{1}H HMQC NMR spectroscopy, which displayed a downfield shift in the ^{195}Pt signal of 205 ppm upon acylation (**Fig. S1**). This large shift indicates a large electronic change at the Pt-center, supporting the modification of the equatorial ammine.

Investigation of the substrate scope revealed that the reaction tolerates a variety of Pt(IV)–ammine and carboxylic acid coupling partners. Modification of the Pt core from cisplatin to carboplatin (**2b**, 37%) or oxaliplatin (**2c**, 65%) was well tolerated, demonstrating the applicability of this method across therapeutically relevant Pt core scaffolds. Additionally, a variety of carboxylic acids could be coupled onto the Pt(IV) core, including those with valuable bioconjugation handles such as maleimide (**2c**, 65%), azide (**2d**, 63%), and alkyne (**2e**, 46%). Moreover, a protected glutamic acid for solid-phase peptide synthesis (**2f**, 50%) was successfully incorporated. Directly bioactive fragments were also successfully coupled to Pt(IV), including biotin (**2g**, 73%) for affinity capture studies, 5-carboxytetramethylrhodamine (5-TAMRA, **2h**, 30%) for fluorescence imaging applications, and small molecule ligands, such as JQ1 (**2i**, 69%).[51]

Incorporation of a 9-fluorenemethyl ester at the apical position of Pt(IV) complexes facilitated a two-step functionalization and deprotection protocol, resulting in Pt(IV)–amide complexes featuring an axial carboxylic acid suitable for subsequent amide coupling (**Fig. 2B**). Complexes with various axial ligands (F^-, Cl^-, $ArCO_2^-$, and 4-tBuPy),[52,53] as well as various Pt cores (cisplatin, carboplatin, and oxaliplatin) were accessed in moderate to good yields (**3a-g**, 18-75%). In addition, functionalization of the Pt core could be accomplished after loading onto a solid support (Sieber amide resin), yielding **4a** and **4b** in moderate yields (**Fig. 2C**, 33% and 37%, respectively) after cleavage from the resin. The ability to tolerate various axial ligands and platinum cores as coupling partners is important for the broad application of the method and utility of the functionalized products. Modulating the primary coordination sphere has a profound impact on the electronic parameters of the Pt(IV) center, which enables fine-tuning of the reduction kinetics of the functionalized products.[54–56]

A solid-state structure of **2i**, obtained via single-crystal X-ray diffraction, provided definitive evidence for modification of the equatorial Pt(IV)–NH_3 ligand (**Fig 3, Fig. S2**). The Pt–NHCO moiety exhibited an X-type Pt–amide bonding structure, characterized by a short C=O bond length of 1.23 Å and long NH–CO bond length of 1.33 Å, consistent with established X-type Pt(IV)–amide complexes.[57–60] The anionic charge of this moiety was neutralized by a triazolium on the JQ1 fragment. From the zwitterionic nature of this structure, it was deduced that the protonated, charge neutral Pt(IV)-complex is relatively acidic and would be deprotonated under neutral pH conditions as the pKa of 1,2,4-triazolium is 2.2.[61] Conversely, other derivatives resulting from ammine functionalization lack an intramolecular base, necessitating protonation of the Pt(IV)–amide for charge balance. Two potential tautomers, L-type amide or imidine configurations, were considered for representing these products. Ground state density functional theory (DFT) calculations[62] indicated that the Pt(IV)–imidine was 3.8 kcal/mol more stable than the corresponding L-type Pt(IV)–amide (**Fig. 3B**). This, in combination with the prevalence of Pt(IV)–imidines characterized crystallographically,[63–68] led to the Pt(IV)–imidine being the preferred tautomer for representation of the protonated, charge-neutral structures.

To demonstrate the utility of these compounds toward mRNA platination, Pt(IV)-ASO constructs targeting enhanced green fluorescent protein (EGFP) mRNA were investigated to optimize reactivity and selectivity. A sense region in the open reading frame of the mRNA was chosen based on two design criteria dictated by the inherent reactivity of platinum towards guanosine: 1) this region featured a "GGG" motif as the intended site of platination, allowing for multiple sites of functionalization and 2) the antisense for this region featured few guanosines, mitigating issues of competing ASO platination. Based on this analysis, an antisense 11-mer PNA was synthesized to this target region by automated flow synthesis via protocols developed in our laboratories.[69,70] To attach Pt to the PNA, a strain-promoted azide-alkyne click strategy was pursued, yielding **nBuPt-PNA$^{369\text{-}379}$** (**Fig. 4A**).

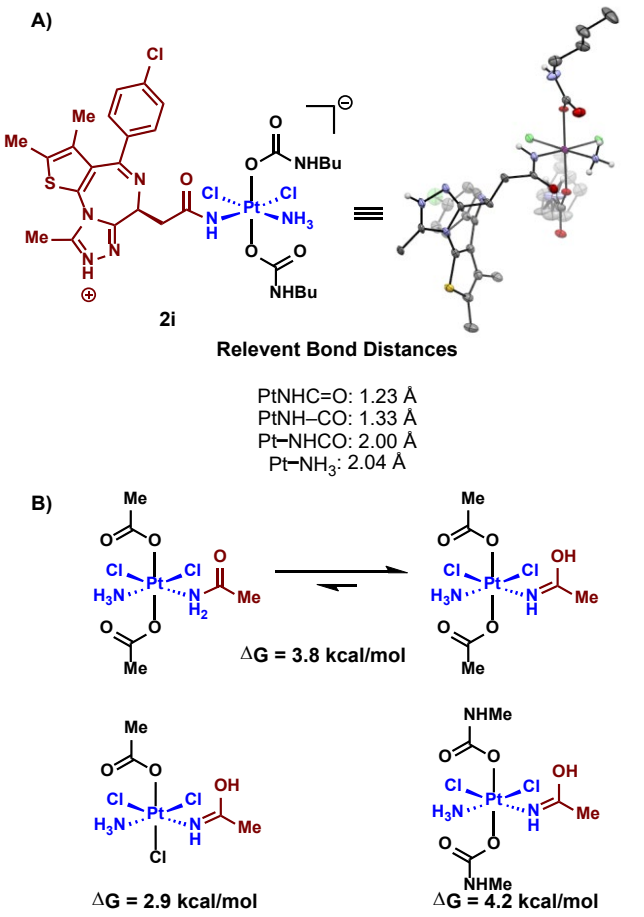

Figure 3. Structural analysis of Pt(IV) complexes by X-ray crystallography and DFT calculations illuminates bonding geometry of products from Pt(IV)-ammine functionalization (A) Solid-state structure of **2i** from single-crystal X-ray diffraction analysis. Thermal ellipsoids are plotted at 50% probability level; solvent omitted for clarity. (B) Optimization of ground-state structures by DFT reveal that the Pt(IV)-imidine tautomer is more stable than the L-type Pt(IV)-amide tautomer by 2.9-4.2 kcal/mol. Geometry and frequency calculations were performed at the PBE0 level of theory with SARC-ZORA-TZVP basis set for Pt and ZORA-def2-SVP for remaining elements (C,N,H,O,Cl) with tight convergence criteria.

Studying the reduction products of **nBuPt-PNA$^{369\text{-}379}$** by liquid chromatography-mass spectrometry (LC-MS) demonstrated that the Pt(II) and the PNA remained attached upon reduction, a key requirement for a successful chemical modification strategy. After incubation of **nBuPt-PNA$^{369\text{-}379}$** with 300 μM sodium ascorbate in PBS for 20 h, a new species was observed by LC-MS, corresponding to a Pt(II)-PNA product, albeit in low conversion (**Fig. 4B**, **Fig. S3**, 9% integrated product peak area). It was hypothesized that the equatorial X-type amide obtained from deprotonation at neutral pH, is a more electron-donating ligand than the starting ammine, resulting in a slow rate of reduction. A series of Pt-PNA constructs were synthesized with electron-withdrawing axial ligands to counteract this increase in electron density at the platinum center. **ArPt-PNA$^{369\text{-}379}$** and **Cl-Pt-PNA$^{369\text{-}379}$** led to significantly more facile reduction, where **ClPt-PNA$^{369\text{-}379}$** was found to be fully reduced to the Pt(II)-PNA by the same LC-MS analysis. The observation of the correct mass/charge ratio of the Pt(II)-PNA, as well as the agreement between the observed and simulated isotopic splitting patterns for a Pt-containing species (**Fig. S4**) provided definitive evidence for the Pt(II) remaining attached to the PNA upon reduction. This was an encouraging indication that these constructs could be used for targeted platination of nucleic acids.

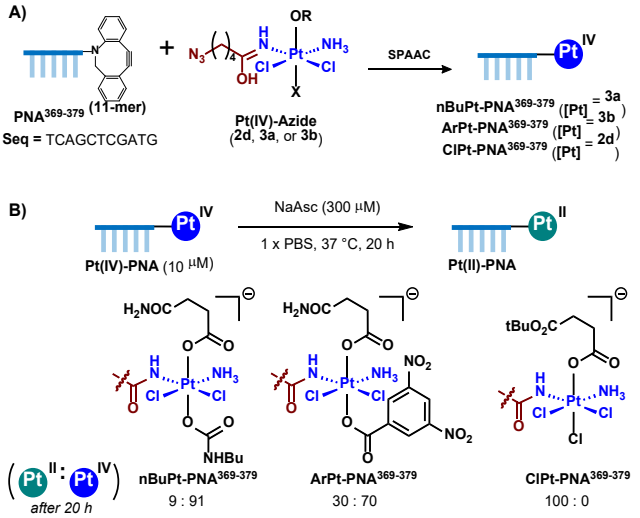

Figure 4. Reduction of Pt(IV)-PNAs is influenced by axial group identity. (A) Accessing Pt(IV)-PNAs via SPAAC reaction. (B) Effect of axial leaving group identity of Pt(IV)-ASO on ease of reduction by sodium ascorbate (NaAsc). Ratios were determined by integrating total ion count area of LC-MS spectra.

To confirm RNA functionalization and characterize the resulting products, the reactivity of **nBuPt-PNA$^{369\text{-}379}$**, **ArPt-PNA$^{369\text{-}379}$**, and **ClPt-PNA$^{369\text{-}379}$** with a 21-mer RNA fragment was examined. This fragment represents a condensed segment of interest within the EGFP mRNA (**Fig. 5A**). After incubation of this series of Pt-PNAs with 21-mer RNA, agarose gel electrophoresis of the reaction mixtures displayed two new species. One species was assigned to be the Pt(IV)-PNA/RNA duplex due to its similar mobility to the Ac-PNA/RNA duplex. Upon reduction of the Pt(IV), the resulting Pt(II) acquires a positive charge after hydrolysis. This allowed for tentative assignment of the slowest mobility species as the Pt(II)-PNA/RNA, as it would have a less negative charge than the corresponding Pt(IV)-containing duplex (**Fig. 5B**). Of note, the more rapidly reducing construct (**ClPt-PNA$^{369\text{-}379}$**) demonstrated significant reactivity towards forming the Pt(II)-PNA/RNA duplex. While the lower mobility of this species is consistent with the generation of a cationic platinum complex, an important mechanistic question remained as to whether the Pt(II) covalently modified the RNA or generated undesired intramolecular PNA platination products.

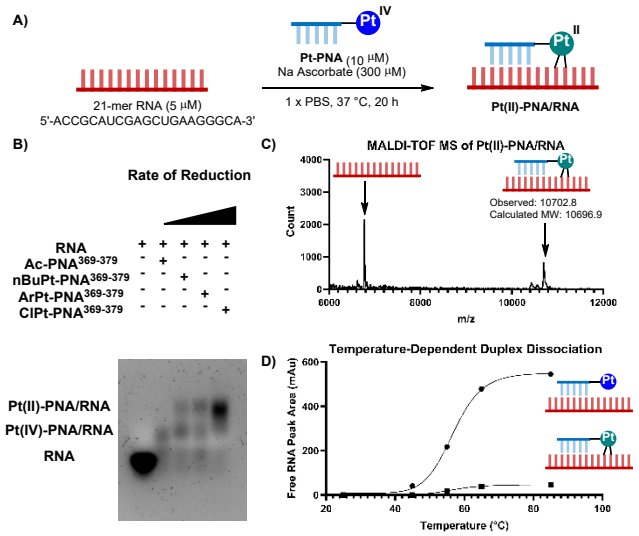

Figure 5. Pt(IV)-PNAs functionalize RNA covalently. (A) Overall reaction scheme between 21-mer RNA and Pt(IV)-PNA constructs under reductive conditions. (B) Examination of reactivity between RNA (5 μM) and Pt(IV)-PNAs (10 μM) with varying axial leaving groups. Analysis of reaction mixtures by agarose gel electrophoresis consistent with formation of Pt(II)-PNA/RNA duplex upon reduction of Pt(IV)-PNA/RNA. Order of rates of reduction determined from **Fig. 4B** (C) MALDI-TOF MS of RNA functionalized by **ClPt-PNA$^{369\text{-}379}$**. (D) Melt curve of Pt(IV)-PNA/RNA duplex and Pt(II)-PNA/RNA duplex obtained from UHPLC by varying column temperature and integration of free RNA at 280 nm.

Evidence for the covalent modification of the RNA was obtained by isolation of the Pt(II)-PNA/RNA product by ultra high-performance liquid chromatography (UHPLC), and observation of its corresponding mass by Matrix Assisted Laser Desorption/Ionization-Time of Flight (MALDI-TOF) MS (**Fig. 5C**). Control duplexes of **Ac-PNA$^{369\text{-}379}$**/RNA and unreduced **ClPt-PNA$^{369\text{-}379}$**/RNA readily disassociated in the mass spectrometer (**Fig. S5**), indicating that the observation of the combined mass was due to an interaction between the Pt(II)-PNA and RNA stronger than base-pairing alone. Additional evidence of covalently modified RNA was obtained via a melting temperature study using UHPLC, where the melting temperatures of the two duplexes were determined by varying the column temperature and integrating the free RNA peak (measured at 280 nm) observed with rising temperature (**Fig. 5D**). This assay demonstrated that the Pt(II)-PNA/RNA duplex remained stable upon heating to 85 °C, while non-covalently bound Pt(IV)-PNA/RNA featured a T_m of ~55 °C. It was further substantiated that this behavior resulted from a Pt-RNA covalent bond by extracting the platinum atom from the Pt(II)-PNA/RNA duplex by treating with KCN (**Fig. S6**). This method, known for sequestering platinum lesions from nucleic acids, serves to dissociate any Pt-RNA bonds.[71,72] After treatment, the resulting PNA/RNA duplex readily dissociated upon heating, supporting the conclusion that Pt(II) is acting as a covalent linkage between the PNA and RNA. Reactivity was not observed between **ClPt-PNA$^{369\text{-}379}$** and a 15-mer RNA with a scrambled binding region (**Fig. S7**). This lack of functionalization of the mismatched RNA, as well as the selective functionalization of the matched RNA in a competition assay format demonstrate that the specificity of the PNA is crucial for selective covalent modification of RNA (**Fig. S8**).

Extension of this reactivity to full-length mRNA (996 nucleotides) demonstrated dose-dependent platination consistent with site-directed functionalization and mRNA silencing (**Fig. 6**). After incubation of EGFP mRNA with **ClPt-PNA$^{369\text{-}379}$** (0–8 equiv.), agarose gel electrophoresis displayed relatively little change in the mRNA mobility across the series (**Fig. S9**). To differentiate covalently modified mRNA from unmodified mRNA, reverse-transcription was performed on the reaction mixtures. It was hypothesized that the covalently attached Pt-PNA lesion would serve to halt reverse-transcription, resulting in truncated cDNA/RNA duplexes as compared to unmodified mRNA. Gel electrophoresis of the reverse-transcribed products demonstrated a dose-dependent decrease in full-length cDNA/RNA duplex and the appearance of truncated cDNA/RNA. This result is consistent with site-directed functionalization of the mRNA and demonstrates that the Pt serves as a lesion, effectively modifying the mRNA. Control complexes of the slower reducing **nBuPt-PNA$^{369\text{-}379}$**, **Ac-PNA$^{369\text{-}379}$**, as well as a scramble **ClPt-PNA$^{369\text{-}379}$** demonstrated no mRNA reactivity (**Fig. S10**), indicating that the synergy between the platinum reactivity and the specificity of the ASO is critical for mRNA functionalization.

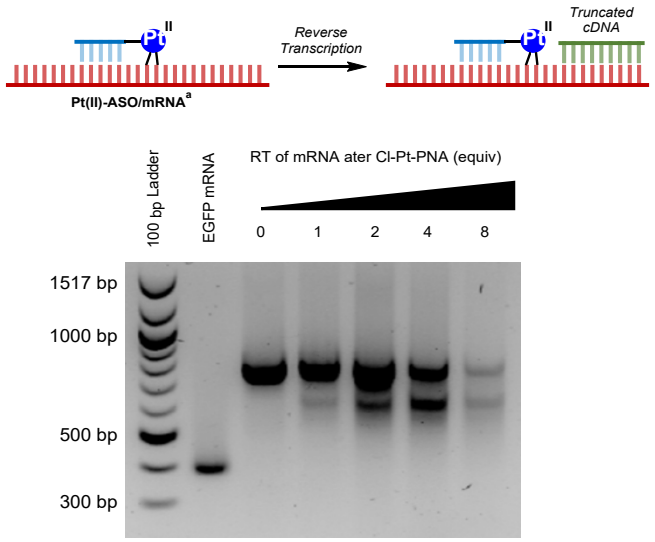

Figure 6. Reverse transcription reveals functionalization of mRNA by **ClPt-PNA$^{369\text{-}379}$**. [a]Conditions for functionalizing mRNA: EGFP mRNA (100 nM, 1 equiv), **ClPt-PNA$^{369\text{-}379}$** (0-8 equiv), RNase inhibitor (5%), sodium ascorbate (300 μM), 1x PBS, rt, 20 h.

Sanger sequencing was performed on double-stranded cDNA obtained from the truncated mRNA/cDNA duplex to determine the site of modification. This analysis revealed that the site of modification was ~120 nucleotides downstream of the PNA's antisense region and the intended site of modification (**Fig. S11**). To understand this discrepancy between the predicted and experimentally determined sites of modification, the structure of the PNA-bound mRNA was simulated using mFold (**Fig. S12**).[73] This structure featured an internal stem loop at the target region, where the intended site of modification is base-paired with a region ~110 nucleotides downstream, corroborating the sequencing results.

The selectivity of the Pt-mediated mRNA silencing was confirmed and quantified by a competition assay between EGFP

mRNA (50 pM) and 1000 equivalents of RNA. In this assay, target and off-target modification were quantified by RT-qPCR, where modification of housekeeping genes (GAPDH and β-actin) were used as representative off-target RNA. EGFP mRNA was effectively silenced by **ClPt-PNA$^{369\text{-}379}$** (IC_{50} = 10.1 ± 6.2 nM) with minimal off-target silencing (**Fig. 7A**). Control compound **Ac-PNA$^{369\text{-}379}$** resulted in no mRNA knockdown (**Fig. S13**), further demonstrating that the Pt-linkage to the mRNA is required for silencing. While **ClPt-PNA$^{369\text{-}379}$** demonstrates good reactivity and selectivity in this assay, the construct exhibited poor water solubility.

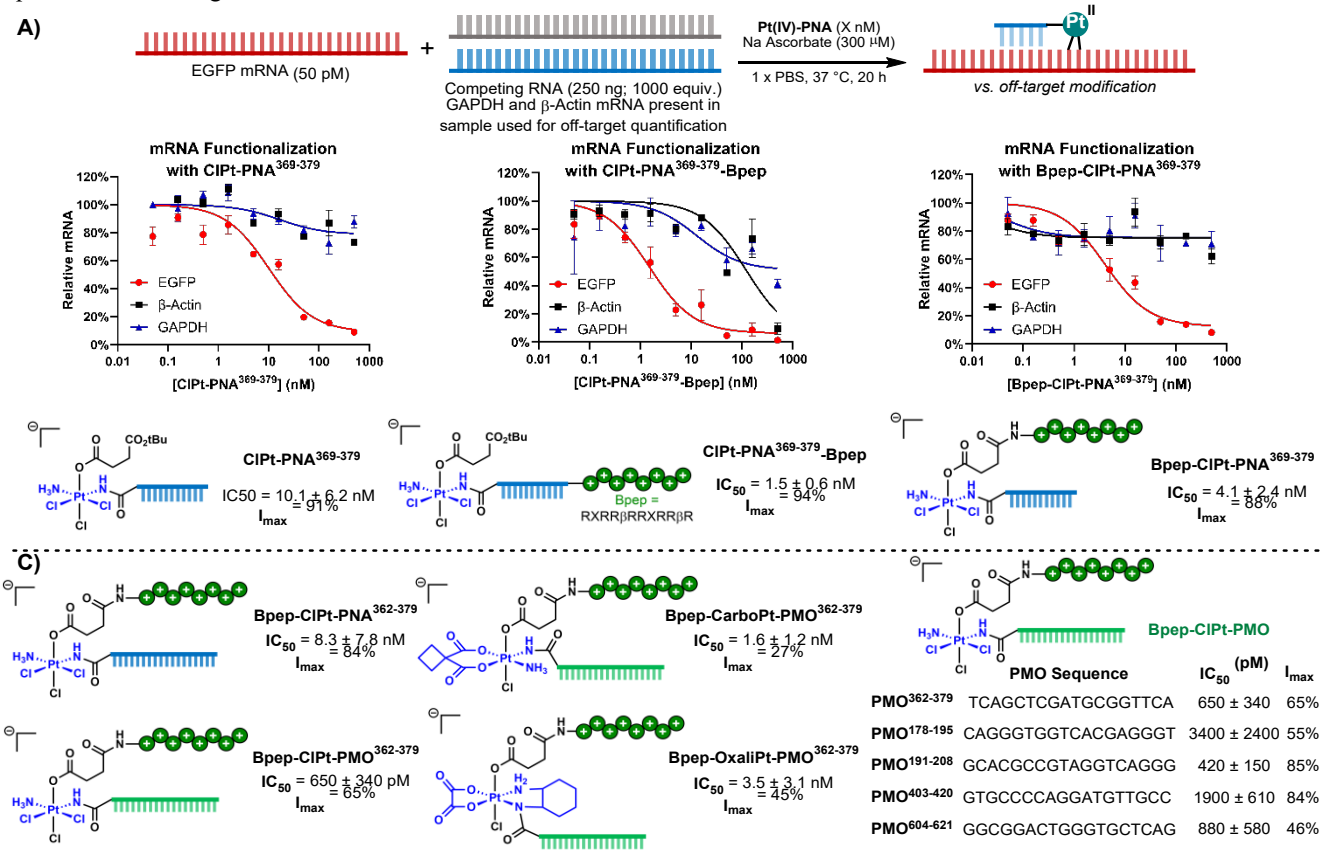

Figure 7. Pt(IV)-ASO constructs selectively functionalize EGFP mRNA in presence of competing RNA. (A) Effect of Bpep addition and connectivity on reactivity and selectivity. (B) Reactivity of a library of Bpep-[Pt]-ASO constructs. EGFP mRNA (50 pM) and competing RNA (1,000 equiv.) were incubated with Pt(IV)-PNA constructs (0 - 500 nM) in 300 μM sodium ascorbate in PBS for 20 h. For Pt(IV)-PMO constructs, 5 pM EGFP mRNA and 10,000 equiv of RNA were used due to lower IC_{50} of Pt(IV)-PMO constructs. Target (EGFP) vs. off-target (β-Actin and GAPDH present in competing RNA) modification was measured by RT-qPCR relative to untreated control. Bars represent the standard deviation of the mean based on n= 3 replicates. IC_{50} and I_{max} values were determined through non-linear fitting in GraphPad Prism

To improve the solubility of this construct, Bpep, an arginine rich peptide,[74] was appended to the C-term of the PNA. This water-soluble construct (**ClPt-PNA$^{369\text{-}379}$-Bpep**) demonstrated improved activity towards EGFP mRNA knockdown (IC_{50} = 1.5 ± 0.6 nM) but also functionalized off-target genes at higher concentrations (>50 nM). It was hypothesized that the highly cationic Bpep was non-specifically interacting with RNA, resulting in non-selective reactivity of the Pt(II) center. To alleviate the off-target effects of the cationic tag, the connectivity of the construct was rearranged to display the Bpep on the axial position of the Pt center. This design would take advantage of the inherent reactivity of Pt(IV) to dissociate its axial ligands upon reduction, thereby decoupling the Pt reactivity from the unselective binding of the Bpep tag. After solution-phase conjugation of **4a** to Bpep and subsequent SPAAC reaction with DBCO-PNA, the resulting **Bpep-ClPt-PNA$^{369\text{-}379}$** construct demonstrated superior reactivity for EGFP mRNA, with an IC_{50} of 4.1 ± 2.4 nM. Importantly, no functionalization of off-target genes was observed with treatment of up to 500 nM construct.

Based on these results, a library of Bpep-Pt-ASOs was synthesized to probe structure-activity relationships (**Fig. 7B**), with ASO architecture being the first parameter of examination. Extending the PNA to an 18-mer PNA (**Bpep-ClPt-PNA$^{362\text{-}379}$**) resulted in a slightly decreased activity, with an IC_{50} of 8.3 ± 7.8 nM. Modifying the 18-mer PNA to the 18-mer PMO architecture (**Bpep-ClPt-PMO$^{362\text{-}379}$**) resulted in a significantly improved IC_{50} of 650 ± 260 pM, while the control compound (**Bpep-PMO$^{362\text{-}379}$**) exhibited no mRNA functionalization (**Fig. S14**). While the Pt(IV)-PMO construct demonstrated superior potency for the target sequence than the corresponding Pt(IV)-PNA, maximum knockdown (I_{max}) of the Pt-PMO construct was significantly lower than that of Pt-PNA construct (65% vs 84%

knockdown, respectively). The effect of the Pt(II) precursor core structure on reactivity was examined via synthesis of **Bpep-CarboPt-PMO$^{362-379}$** and **Bpep-OxaliPt-PMO$^{362-379}$**, although these constructs yielded inferior IC_{50} and I_{max} values.

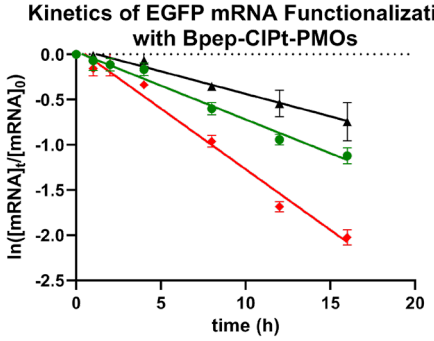

	k (s^{-1})	$t_{1/2}$ (nours)
Bpep-ClPt-PMO$^{178-195}$	0.050	14
Bpep-ClPt-PMO$^{362-379}$	0.075	9.3
Bpep-ClPt-PMO$^{191-208}$	0.134	5.2

Figure 8. Kinetics of EGFP mRNA functionalization by Bpep-ClPt-PMO are affected by the ASO sequence. Functionalization of EGFP mRNA (5 pM) by Pt-PMO constructs (50 nM) in the presence of competing RNA (10,000 equiv.) was measured by RT-qPCR (standard conditions from **Fig. 6B**) relative to t = 0 h. Bars represent the standard deviation of the mean based on n= 3 replicates.

A variety of Bpep-ClPt-PMO constructs were synthesized to examine the effect of mRNA target region on mRNA reactivity. Regions of high binding affinity were selected based on a computational screening approach[75,76] (**Fig. S15**). This series of constructs provided varied IC_{50} values, with the construct **Bpep-ClPt-PMO$^{191-208}$** demonstrating an improved IC_{50} of 420 ± 150 pM. While the range of IC_{50} values (420 to 3400 pM) obtained by changing the ASO sequence could be explained by an effect of ASO sequence on binding thermodynamics and kinetics, the varying I_{max} (46 to 85%) was initially surprising.

To understand the origin of the divergence in I_{max} values, time-dependent reactivity studies of constructs based on PMO$^{178-195}$, PMO$^{191-208}$, and PMO$^{362-379}$ were undertaken. It was observed that the functionalization of mRNA by all constructs followed first order decay kinetics with varying rate constants (**Fig. 8**). These marked differences in rates suggest that the platination of the mRNA by the reduced Pt(II)-ASO is rate-determining, where the rate of this functionalization is influenced by changing the target region in the mRNA, allowing for tuning of the functionalization kinetics. A mechanism where reduction of the Pt(IV) is rate-determining was rejected by observation that the reaction is 0th order in reductant (**Fig. S16**). Taken together, a combined proposed mechanism features an initial equilibrium binding event, forming a Pt(IV)-ASO/mRNA duplex. The Pt(IV) then undergoes exergonic reduction, furnishing a Pt(II)-ASO/mRNA duplex. This duplex then undergoes rate-determining crosslinking, resulting in the covalent modification of the mRNA.

Conclusions

In summary, we have developed a late-stage functionalization strategy for coupling of carboxylic acids to the ammine position of Pt(IV)-prodrugs. This reaction was tolerant to numerous coupling partners, including various Pt-prodrugs with different Pt(II)-cores and with varying axial leaving groups. A variety of carboxylic acids could be employed, including those with valuable conjugation handles and bioactive motifs. Functionalized products with pendant azides could be readily coupled to ASOs via SPAAC to generate Pt(IV)-ASO constructs, which after tuning of the reduction rate via varying the axial ligand, could covalently modify both short RNA fragments and mRNA. Covalent modification was demonstrated via electrophoretic mobility shift assay, temperature-dependent dissociation assay, MALDI-TOF MS, and RT-qPCR.

Pt(IV)-ASO constructs were selective for the gene of interest in the presence of 1,000-10,000 equivalents of competing RNA, with an IC_{50} of 10.1 ± 4.6 nM for initial construct **ClPt-PNA$^{369-379}$**. Several rounds of optimization were performed, including 1) addition of Bpep to the axial position of the Pt to solubilize the construct, 2) changing the ASO to a PMO to improve IC_{50}, and 3) optimizing the sequence of the PMO to further improve IC_{50} and I_{max}. The resulting **Bpep-ClPt-PMO$^{191-208}$** demonstrated an IC_{50} of 420 pM with an I_{max} of 85% with no off-target functionalization of competing RNA. Mechanistic studies revealed that the rate-determining step of the reaction was covalent modification of the mRNA by the Pt(II), where the rate of this reaction was strongly affected by the PMO sequence. The Pt(IV)-ASO platform offers an approach to covalently modify nucleic acids, including RNA and mRNA as well as potential compatibility with DNA, siRNA and miRNA, thereby expanding the chemical space for ASO design and unlocking opportunities in molecular biology research.

Notes

The authors declare no competing financial interests.

ACKNOWLEDGMENT

We gratefully acknowledge the National Cancer Institute (R01-CA237063) for financial support. E.M. was supported by a postdoctoral fellowship from the Ludwig Center at MIT's Koch Institute for Integrative Cancer Research. We thank Dr. Peter Mueller for X-ray crystallographic analysis and Dr. Gino Occhialini for assistance with geometry optimization by DFT. We also thank Dr. Simon Rössler, Dr. Nathalie Grob, Ching-Pei Hsu, Dr. Nate Dow, Dr. Giulio Fittolani, and Dr. Stephen Byrne for helpful discussions.

REFERENCES

(1) Jaroszewicz, W.; Morcinek-Orłowska, J.; Pierzynowska, K.; Gaffke, L.; Węgrzyn, G. Phage Display and Other Peptide Display Technologies. *FEMS Microbiol Rev* **2022**, *46*, 1–25.

(2) Quartararo, A. J.; Gates, Z. P.; Somsen, B. A.; Hartrampf, N.; Ye, X.; Shimada, A.; Kajihara, Y.; Ottmann, C.; Pentelute, B. L. Ultra-Large Chemical Libraries for the Discovery of High-Affinity Peptide Binders. *Nat Commun* **2020**, *11*, 1–11.

(3) Takahashi, T. T.; Austin, R. J.; Roberts, R. W. mRNA Display: Ligand Discovery, Interaction Analysis and Beyond. *Trends Biochem Sci* **2003**, *28*, 159–165.

(4) Gironda-Martínez, A.; Donckele, E. J.; Samain, F.; Neri, D. DNA-Encoded Chemical Libraries: A Comprehensive Review

with Succesful Stories and Future Challenges. *ACS Pharmacol Transl Sci* **2021**, *4*, 1265–1279.

(5) Boutureira, O.; Bernardes, G. J. L. Advances in Chemical Protein Modification. *Chem Rev* **2015**, *115*, 2174–2195.

(6) Zhao, L.; Zhao, J.; Zhong, K.; Tong, A.; Jia, D. Targeted Protein Degradation: Mechanisms, Strategies and Application. *Signal Transduct Target Ther* **2022**, *7, 113*.

(7) Dhuri, K.; Bechtold, C.; Quijano, E.; Pham, H.; Gupta, A.; Vikram, A.; Bahal, R. Antisense Oligonucleotides: An Emerging Area in Drug Discovery and Development. *J Clin Med* **2020**, *9*, 1–24.

(8) Matsukura, M.; Shinozukat, K.; Zont, G.; Mitsuya, H.; Reitz, M.; Cohent, J. S.; Broder, S. Phosphorothioate Analogs of Oligodeoxynucleotides: Inhibitors of Replication and Cytopathic Effects of Human Immunodeficiency Virus. *Medical Sciences* **1987**, *84*, 7706–7710.

(9) Agrawal, S.; Goodchild, J.; Civeirat, M. P.; Thorntont, A. H.; Sarint, P. S.; Zamecnik, P. C. *Oligodeoxynucleoside Phosphoramidates and Phosphorothioates as Inhibitors of Human Immunodeficiency Virus*; 1988; Vol. 85.

(10) Furdon, P. J.; Dominski, Z.; Kole, R. Nucleic Acids Research RNase H Cleavage of RNA Hybridized to Oligonucleotides Containing Methylphosphonate, Phosphorothioate and Phosphodiester Bonds. *Nucleic Acids Res.* **1989**, *17*, 9193–9204.

(11) Eckstein, F. Phosphorothioate Oligodeoxynucleotides : What Is Their Origin and What Is Unique About Them? *Antisense Nucleic Acid Drug Dev* **2000**, *10*, 117–121.

(12) Koshkin, A. A.; Singh, S. K.; Nielsen, P.; Rajwanshi, V. K.; Kumar, R.; Meldgaard, M.; Olsen, C. E.; Wengel, J. LNA (Locked Nucleic Acids): Synthesis of the Adenine, Cytosine, Guanine, 5-Methylcytosine, Thymine and Uracil Bicyclonucleoside Monomers, Oligomerisation, and Unprecedented Nucleic Acid Recognition. *Pergamon Tetrahedron* **1998**, *54*, 3607–3630.

(13) Obika, S.; Nanbu, D.; Hari, Y.; Andoh, J.-I.; Morio, K.-I.; Doi, T.; Imanishi, T. Stability and Structural Features of the Duplexes Containing Nucleoside Analogues with a Fixed N-Type Conformation, 2'-O,4'-C-Methyleneribonucleosides. *Tetrahedron Lett* **1998**, *39*, 5401–5404.

(14) Braasch, D. A.; Corey, D. R. Locked Nucleic Acid (LNA): Fine-Tuning the Recognition of DNA and RNA. *Chem. Biol.* **2001**, *8*, 1–7.

(15) Manoharan, M. 2'-Carbohydrate Modifications in Antisense Oligonucleotide Therapy: Importance of Conformation, Configguration and Conjugation. *Biochim Biophys Acta* **1999**, *1489*, 117–130.

(16) Mangos, M. M.; Damha, M. J. Flexible and Frozen Sugar-Modified Nucleic Acids-Modulation of Biological Activity Through Furanose Ring Dynamics in the Antisense Strand. *Curr Top Med Chem* **2002**, *2*, 1147–1171.

(17) Egli, M.; Minasov, G.; Tereshko, V.; Pallan, P. S.; Teplova, M.; Inamati, G. B.; Lesnik, E. A.; Owens, S. R.; Ross, B. S.; Prakash, T. P.; Manoharan, M. Probing the Influence of Stereoelectronic Effects on the Biophysical Properties of Oligonucleotides: Comprehensive Analysis of the RNA Affinity, Nuclease Resistance, and Crystal Structure of Ten 2′-O-Ribonucleic Acid Modifications. *Biochemistry* **2005**, *44*, 9045–9057.

(18) Prakash, T. P. An Overview of Sugar-Modified Oligonucleotides for Antisense Therapeutics. *Chem Biodivers* **2011**, *8*, 1616–1641.

(19) Freier, S. M.; Altmann, K.-H. The Ups and Downs of Nucleic Acid Duplex Stability: Structure-Stability Studies on Chemically-Modified DNA:RNA Duplexes. *Nucleic Acids Res.* **1997**, *25*.

(20) Crooke, S. T. Molecular Mechanisms of Antisense Oligonucleotides. *Nucleic Acid Ther* **2017**, *27*, 70–77.

(21) Gagliardi, M.; Ashizawa, A. T. The Challenges and Strategies of Antisense Oligonucleotide Drug Delivery. *Biomedicines* **2021**, *9*, 433

(22) Moser, H. E. Sequence-Selective Recognition of DNA by Strand with a Thymine-Substituted Polyamide. *Proc. Natl. Acad. Sci. U.S.A* **1990**, *87*, 2984.

(23) Pellestor, F.; Paulasova, P. The Peptide Nucleic Acids (PNAs), Powerful Tools for Molecular Genetics and Cytogenetics. *European Journal of Human Genetics* **2004**, *12*, 694–700.

(24) Summerton, J.; Weller, D. Morpholino Antisense Oligomers: Design, Preparation, and Properties. *Antisense Nucleic Acid Drug Dev* **1997**, *7*, 187–195.

(25) Heo, Y. A. Golodirsen: First Approval. *Drugs* **2020**, *80*, 329–333.

(26) Syed, Y. Y. Eteplirsen: First Global Approval. *Drugs* **2016**, *76*, 1699–1704.

(27) Dhillon, S. Viltolarsen: First Approval. *Drugs* **2020**, *80*, 1027–1031.

(28) Hudziak, R. M.; Barofsky, E.; Barofsky, D. F.; Weller, D. L.; Huang, S.-B.; Weller1, D. D. Resistance of Morpholino Phosphorodiamidate Oligomers to Enzymatic Degradation. *Antisense Nucleic Acid Drug Dev* **1996**, *6*, 267–272.

(29) Sakamoto, T.; Shigeno, A.; Ohtaki, Y.; Fujimoto, K. Photo-Regulation of Constitutive Gene Expression in Living Cells by Using Ultrafast Photo-Cross-Linking Oligonucleotides. *Biomater Sci* **2014**, *2*, 1154–1157.

(30) Hennessy, J.; McGorman, B.; Molphy, Z.; Farrell, N. P.; Singleton, D.; Brown, T.; Kellett, A. A Click Chemistry Approach to Targeted DNA Crosslinking with Cis-Platinum(II)-Modified Triplex-Forming Oligonucleotides. *Angewandte Chemie - International Edition* **2022**, *61*

(31) Rottenberg, S.; Disler, C.; Perego, P. The Rediscovery of Platinum-Based Cancer Therapy. *Nat Rev Cancer* **2021**, *21*, 37–50.

(32) Kelland, L. The Resurgence of Platinum-Based Cancer Chemotherapy. *Nat Rev Cancer* **2007**, *7*, 573–584.

(33) Todd, R. C.; Lippard, S. J. Inhibition of Transcription by Platinum Antitumor Compounds. *Metallomics* **2009**, *1*, 280–291.

(34) Johnstone, T. C.; Suntharalingam, K.; Lippard, S. J. The Next Generation of Platinum Drugs: Targeted Pt(II) Agents, Nanoparticle Delivery, and Pt(IV) Prodrugs. *Chem Rev* **2016**, *116*, 3436–3486.

(35) Wee, H. A.; Khalaila, I.; Allardyce, C. S.; Juillerat-Jeanneret, L.; Dyson, P. J. Rational Design of Platinum(IV) Compounds to Overcome Glutathione-S- Transferase Mediated Drug Resistance. *J. Am. Chem. Soc.* **2005**, *127*, 1382–1383.

(36) Yang, J.; Sun, X.; Mao, W.; Sui, M.; Tang, J.; Shen, Y. Conjugate of Pt(IV)-Histone Deacetylase Inhibitor as a Prodrug for Cancer Chemotherapy. *Mol Pharm* **2012**, *9*, 2793–2800.

(37) Ma, L.; Ma, R.; Wang, Y.; Zhu, X.; Zhang, J.; Chan, H. C.; Chen, X.; Zhang, W.; Chiu, S. K.; Zhu, G. Chalcoplatin, a Dual-

(51) Filippakopoulos, P.; Qi, J.; Picaud, S.; Shen, Y.; Smith, W. B.; Fedorov, O.; Morse, E. M.; Keates, T.; Hickman, T. T.; Felletar, I.; Philpott, M.; Munro, S.; McKeown, M. R.; Wang, Y.; Christie, A. L.; West, N.; Cameron, M. J.; Schwartz, B.; Heightman, T. D.; La Thangue, N.; French, C. A.; Wiest, O.; Kung, A. L.; Knapp, S.; Bradner, J. E. Selective Inhibition of BET Bromodomains. *Nature* **2010**, *468* (7327), 1067–1073. https://doi.org/10.1038/nature09504.

(52) Xu, Z.; Chan, H. M.; Li, C.; Wang, Z.; Tse, M. K.; Tong, Z.; Zhu, G. Synthesis, Structure, and Cytotoxicity of Oxaliplatin-Based Platinum(IV) Anticancer Prodrugs Bearing One Axial Fluoride. *Inorg Chem* **2018**, *57* (14), 8227–8235. https://doi.org/10.1021/acs.inorgchem.8b00706.

(53) Zhou, Q.; Chen, S.; Xu, Z.; Liu, G.; Zhang, S.; Wang, Z.; Tse, M. K.; Yiu, S. M.; Zhu, G. Multitargeted Platinum(IV) Anticancer Complexes Bearing Pyridinyl Ligands as Axial Leaving Groups. *Angewandte Chemie - International Edition* **2023**, *62* (18). https://doi.org/10.1002/anie.202302156.

(54) Hambley, T. W.; Battle, A. R.; Deacon, G. B.; Lawrenz, E. T.; Fallon, G. D.; Gatehouse, B. M.; Webster, L. K.; Rainone, S. Modifying the Properties of Platinum(IV) Complexes in Order to Increase Effectiveness. *J. Inorg. Biochem.* **1999**, *77*, 3–12.

(55) Peloso, A. An Investigation on the Influence of Co-Ordinated Aliphatic Amines on the Rates of Reduction of Tetrachlorodiamineplatinum(IV) Complexes. *J. Chem. Soc. Dalton Trans.* **1984**, 249–254.

(56) Yap, S. Q.; Chin, C. F.; Hong Thng, A. H.; Pang, Y. Y.; Ho, H. K.; Ang, W. H. Finely Tuned Asymmetric Platinum(IV) Anticancer Complexes: Structure–Activity Relationship and Application as Orally Available Prodrugs. *ChemMedChem* **2017**, *12* (4), 300–311. https://doi.org/10.1002/cmdc.201600577.

(57) Abo-Amer, A.; Boyle, P. D.; Puddephatt, R. J. Oxidation of a Dimethyl Platinum(II) Complex with Xenon Difluoride: The Important Role of Solvent. *Inorg Chem Commun* **2015**, *61*, 193–196. https://doi.org/10.1016/j.inoche.2015.10.002.

(58) Pelosi, G.; Ravera, M.; Gabano, E.; Fregonese, F.; Osella, D. Unprecedented One-Pot Synthesis of an Unsymmetrical Cisplatin-Based Pt(Iv)-Acetamidato Complex. *Chemical Communications* **2015**, *51* (38), 8051–8053. https://doi.org/10.1039/c5cc02477c.

(59) Liu, F.; Chen, W. Oxidative Addition of Cl2, HClO to Square-Planar PtII Complexes: Synthesis and Structural Characterization of Platinum(II) and Platinum(IV) Bis(Amidate) Complexes. *Eur J Inorg Chem* **2006**, No. 6, 1168–1173. https://doi.org/10.1002/ejic.200500878.

(60) Ravera, M.; Gabano, E.; Zanellato, I.; Fregonese, F.; Pelosi, G.; Platts, J. A.; Osella, D. AntiproliferatIVe ActIVity of a Series of Cisplatin-Based Pt(IV)-Acetylamido/Carboxylato Prodrugs. *Dalton Transactions* **2016**, *45* (12), 5300–5309. https://doi.org/10.1039/c5dt04905a.

(61) Garratt, P. J. 1,2,4-Triazoles. In *Comprehensive Heterocyclic Chemistry II*; 1996; pp 127–163.

(62) Debefve, L. M.; Pollock, C. J. Systematic Assessment of DFT Methods for Geometry Optimization of Mononuclear Platinum-Containing Complexes. *Physical Chemistry Chemical Physics* **2021**, *23* (43), 24780–24788. https://doi.org/10.1039/d1cp01851e.

(63) Chernyshev, A. N.; Bokach, N. A.; Gushchin, P. V.; Haukka, M.; Kukushkin, V. Y. Reactions of Platinum(Iv)-Bound Nitriles with Isomeric Nitroanilines: Addition vs. Substitution. *Dalton Transactions* **2012**, *41* (41), 12857–12864. https://doi.org/10.1039/c2dt30986f.

(64) Luzyanin, K. V.; Haukka, M.; Bokach, N. A.; Kuznetsov, M. L.; Kukushkin, V. Y.; Pombeiro, A. J. L. Platinum(IV)-Mediated Hydrolysis of Nitriles Giving Metal-Bound Iminols. *Journal of the Chemical Society, Dalton Transactions* **2002**, 9, 1882–1887. https://doi.org/10.1039/b108327a.

(65) Gonzalez, A. M.; Cini, R.; Intini, F. P.; Pacifico, C.; Natile, G. X-Ray Structures of the First Platinum Complexes with Z Configuration Iminoether Ligands: Trans-Dichlorobis(1-Imino-1-Methoxy-2,2′dimethylpropane)Platinum(II) and Trans-Tetrachlorobis(1-Imino-1methoxy-2,2′-Dimethylpropane)Platinum(IV). *Inorg Chem* **2002**, *41*, 470–478.

(66) Zhang, F.; Broczkowski, M. E.; Jennings, M. C.; Puddephatt, R. J. Oxidative Addition Chemistry of Dimethyl(Dipyridyl Ketone)Platinum(II). *Can J Chem* **2005**, *83*, 595–605.

(67) Bokach, N. A.; Kukushkin, V. Y.; Kuznetsov, M. L.; Garnovskii, D. A.; Natile, G.; Pombeiro, A. J. L. Direct Addition of Alcohols to Organonitriles Activated by Ligation to a Platinum(IV) Center. *Inorg Chem* **2002**, *41*, 2041–2053.

(68) Chulkova, T. G.; Gushchin, P. V.; Haukka, M.; Kukushkin, V. Y. 18-Crown-6 as a Linker for (Imino Ester)2Pt Centers Providing Their Assembly into 1D Arrays via Hydrogen Bonding. *Inorg Chem Commun* **2010**, *13*, 580–583.

(69) Li, C.; Callahan, A. J.; Phadke, K. S.; Bellaire, B.; Farquhar, C. E.; Zhang, G.; Schissel, C. K.; Mijalis, A. J.; Hartrampf, N.; Loas, A.; Verhoeven, D. E.; Pentelute, B. L. Automated Flow Synthesis of Peptide-PNA Conjugates. *ACS Cent Sci* **2022**, *8*, 205–213.

(70) Li, C.; Callahan, A. J.; Simon, M. D.; Totaro, K. A.; Mijalis, A. J.; Phadke, K. S.; Zhang, G.; Hartrampf, N.; Schissel, C. K.; Zhou, M.; Zong, H.; Hanson, G. J.; Loas, A.; Pohl, N. L. B.; Verhoeven, D. E.; Pentelute, B. L. Fully Automated Fast-Flow Synthesis of Antisense Phosphorodiamidate Morpholino Oligomers. *Nat Commun* **2021**, *12*.

(71) Bauer, W.; Gonias, S. L.; Kam, S. K.; Wu, K. C.; Stephen J. Lippard. Binding of the Antitumor Drug Platinum Uracil Blue to Closed and Nicked Circular Duplex DNAs. *Biochemistry* **1978**, *17*, 1060–1068.

(72) Lippard, S. J.; Hoeschelet, J. D. Binding of Cis-and Trans-Dichlorodiammineplatinum(II) to the Nucleosome Core. *Proc. Natl. Acad. Sci. USA* **1979**, *76*, 6091–6095.

(73) Zuker, M. Mfold Web Server for Nucleic Acid Folding and Hybridization Prediction. *Nucleic Acids Res.* **2003**, *31*, 3406–3415.

(74) Fadzen, C. M.; Holden, R. L.; Wolfe, J. M.; Choo, Z. N.; Schissel, C. K.; Yao, M.; Hanson, G. J.; Pentelute, B. L. Chimeras of Cell-Penetrating Peptides Demonstrate Synergistic Improvement in Antisense Efficacy. *Biochemistry* **2019**, *58*, 3980–3989.

(75) Walton, S. P.; Stephanopoulos, G. N.; Yarmush, M. L.; Roth, C. M. Prediction of Antisense Oligonucleotide Binding Affinity to a Structured RNA Target. *Biotechnol Bioeng* **1999**, *65*, 1–9.

(76) Patrick Walton, S.; Stephanopoulos, G. N.; Yarmush, M. L.; Roth, C. M. Thermodynamic and Kinetic Characterization of Antisense Oligodeoxynucleotide Binding to a Structured MRNA. *Biophys J* **2002**, *82*, 366–377.